Reprinted from the Journal of the American Ceramic Society, Vol. 66, No. 5, May 1983

Theory of Fatigue for Brittle Flaws Originating from Residual Stress Concentrations

EDWIN R. FULLER* and BRIAN R. LAWN*

Fracture and Deformation Division, National Bureau of Standards, Washington, DC 20234

ROBERT F. COOK*

Department of Applied Physics, School of Physics, University of New South Wales, New South Wales 2033, Australia

A theory is formulated for the general fatigue response of brittle flaws which experience residual stress concentrations. The indentation crack is taken as a model flaw system for the purpose of setting up the basic fracture mechanics equations, but the essential results are expected to have a wider range of applicability in the strength characterization of ceramics. A starting fatigue differential equation is first set up by combining an appropriate stress intensity factor for point- or line-contact flaws with a power-law crack velocity function. Analytical solutions are then obtained for the case of static fatigue. The resulting relation between lifetime and failure stress is shown to have exactly the same power-law form as the conventional solution for Griffith (residual-stress-free) flaws. This "equivalence" is used as a basis for extending the results to dynamic fatigue. A comparison of these analytical solutions with numerical counterparts defines the limits of accuracy of the theoretical procedure. However, while the form of the lifetime relation remains invariant, the values of the exponent and coefficient differ significantly for flaws with and without residual stress. Accordingly, the application of conventional fatigue theory to evaluate crack velocity parameters, without due regard for the nature of the critical flaw, can lead to serious errors. Explicit conversion formulas are given for transforming "apparent" velocity parameters for indentation flaws directly into "true" parameters. The implications of these results concerning the use of the indentation method for materials evaluation are discussed.

I. Introduction

It is well recognized that the failure of brittle materials is governed by the micromechanics of crack growth from small flaws, and that chemical enhancement of this crack growth can cause significant reductions in the strength with increasing time under load. Embodied in the conventional fracture mechanics approach to "fatigue" phenomena of this kind[1,2] are three underlying assumptions: (*a*) The time dependence of the loading stresses, taken to act uniformly across the prospective crack plane, is specifiable; (*b*) the driving force on the extending crack is uniquely determined at any given characteristic length by these applied loading stresses; (*c*) the rate of crack extension is in turn uniquely determined by some well-defined function of the driving force for any given material/environment system. These assumptions allow one to write down a differential equation in crack length and time, the solution of which defines the stress conditions at failure. The widespread success enjoyed by the fracture mechanics formulation arises from the amenability to solutions in simple, closed form, which provide a convenient basis for lifetime predictions.

Apart from the clear-cut distinction made between loading at constant stress ("static fatigue") and constant stress rate ("dynamic fatigue"), surprisingly little attention has been devoted to the effects that potential variations in the starting equations may have in the lifetime analysis. Wiederhorn and Ritter[3] examined the crack velocity function, and concluded that any of the commonly accepted empirical forms may fit fatigue data equally well (although extrapolations beyond the data range could lead to significant discrepancies in the predictions). Of the assumptions listed above, the second has been subjected to least scrutiny, it generally being assumed, without question, that the flaws respond in the classical "Griffith" sense; that is, the flaw is driven solely by the applied loading, this force increasing monotonically with the crack size until some instability condition is met.[4,5] It is thus implicit in the statement of the problem that any preexisting stresses which may have been responsible for generating the critical flaw in the first place[5,6] have long since ceased to be a significant contributing factor in the net driving force on the system.

However, recent studies of controlled flaws produced by indentation in strength test pieces have demonstrated that residual crack-generation stresses can have a profound influence on the crack evolution to failure.[7] The source of the residual field in this case is elastic-plastic mismatch at the boundary of the deformation zone which encases the sharp point and edges of the contacting body.[8] It then becomes necessary to incorporate a residual-contact term into the fracture mechanics equation for the crack driving force. Characteristically, this contribution *decreases* monotonically with crack size.[8] The resulting expression for the net force on the crack now takes on a considerably more complicated form. This complexity is such that the appropriate fatigue differential equation no longer appears to have simple analytic solutions. Accordingly, the first systematic investigations of residual-stress effects in fatigue, using results from dynamic[9] and static[10] loading tests on Vickers-indented soda-lime glass in water as a data base, were made by obtaining numerical solutions specific to one particular indenter/material/environment system. A subsequent analysis,[11] based on a reformulation of the differential equation in terms of judiciously normalized variables, allowed for generalization of the numerical procedure to include solutions for all possible systems. Most notably, this last study produced an empirical dynamic fatigue relation, for flaws satisfying a power-law crack velocity function, which was indistinguishable in form from that derived analytically for Griffith flaws. The exponents and coefficients in this relation were not, however, identical in the two cases; in particular, the values of the fatigue exponent, which for Griffith flaws is a direct measure of the corresponding exponent in the crack velocity function, differed by some 30%. A case study on a glass-ceramic[12] confirmed these and other features of the residual-stress theory, and outlined several unique advantages of the indentation method as a means for evaluating basic fatigue parameters.

One point that must be made at the outset is that indentation cracks should not be regarded simply as artificially introduced entities which bear no resemblance to strength-controlling flaws in real materials. There is growing evidence that the degrading surface damage which many ceramic components experience in finishing (e.g. machining)[13] or in service (sharp particle impact)[14] are characterized by the same residual stress effects as are indentation flaws. Indeed, the observation of strongly analogous local stress field effects about microstructural flaws in ceramics[15] suggests that the presence of residual crack driving forces may be the rule rather than the exception.

Viewed against this background the solution of the indentation fatigue problem takes on a broader significance. Accordingly, the

Received August 25, 1982; revised copy received December 27, 1982; approved January 3, 1983.
Supported by the Australian Research Grants Committee and the U. S. Office of Naval Research.
*Member, the American Ceramic Society.

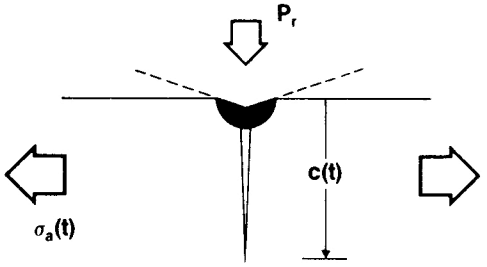

Fig. 1. Indentation flaw; crack of size c is formed at contact load P_r and subsequently subjected to applied tensile stress σ_a. Deformation zone about contact gives rise to residual stress field which contributes to crack driving force.

numerical base of the earlier analyses[9-12] must be seen as restrictive. Ideally, one would like to be able to obtain analytical solutions of the master differential equation in its most general possible form. Such solutions would provide a sounder basis for making intercomparisons between (*a*) flaws of different geometry, e.g. "point" flaws produced in normal loading vs "line" flaws produced in sliding loading; (*b*) different crack velocity functions; (*c*) static vs dynamic fatigue. In this paper we present an analysis which meets this ideal at least in part, the greatest restrictions being the need to retain a power-law crack velocity function and to obtain the dynamic fatigue solutions by an "equivalence" argument. The ensuing fatigue relation between lifetime and failure stress confirms the findings of the previous empirical studies, but now provides more explicit expressions for obtaining crack velocity parameters from fatigue plot slopes and intercepts.

II. Analytical Solution of Fatigue Differential Equation for Constant Applied Stress

(1) The Stress Intensity Factor and the Inert Strength

The key step in generalizing the Griffith-flaw concept to include residual-stress effects is an appropriate expression for the crack driving force. The essential variables expected to appear in any such expression are depicted in Fig. 1: c is the characteristic crack size, P_r the indentation load which determines the level of the residual field, and σ_a the subsequently applied tensile stress which takes the system to failure. In this work we shall make a special distinction between the geometrical extremes of "point" and "line" flaws; the former defines a crack configuration of semicircular profile centered about a point-force contact ($P_r \equiv$force), the latter a crack of straight front parallel to a line-force contact ($P_r \equiv$force/length). We shall also assume that the cracks are "well developed," i.e. are large compared to the deformation zone from which these cracks initiate. Following our previous procedure,[11] the requisite crack driving force may be formulated in terms of the composite stress intensity factor

$$K = K_r + K_a \tag{1a}$$

where the terms

$$K_r = \chi_r P_r / c^{r/2} \tag{1b}$$

$$K_a = \psi_r \sigma_a c^{1/2} \tag{1c}$$

respectively represent the contributions from the residual contact field and the applied loading: here $r=3$ for point flaws and $r=1$ for line flaws; χ_r and ψ_r are dimensionless parameters of the indentation stress field and the crack geometry, respectively. This formulation is subject to some modification due to the influence of such factors as secondary crack systems, spurious surface stress states, etc.; detailed discussion of these factors is available elsewhere,[11] and will consequently be pursued no further here.

Equation (1) has certain features which are pertinent to the fatigue analysis to follow. These features are evident in the plots of the function $K(c)$ in Fig. 2 for both point and line flaws. The curves for fixed values of P_r and σ_a pass through a well-defined

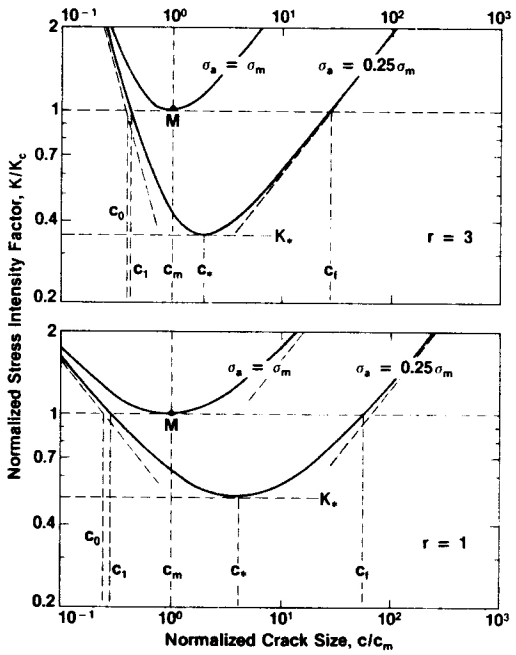

Fig. 2. Stress intensity factor as function of crack size (Eq. (1)) for point ($r=3$) and line ($r=1$) flaws. Inclined broken lines represent individual residual and applied components (Eqs. (1*b*) and (1*c*)); solid curves represent composite functions.

minimum, tending asymptotically on either side of this minimum to plots of the residual component of the stress intensity factor in the small-crack limit and of the applied component in the large-crack limit. The coordinate variables are normalized to the reference points M, which are of special significance in establishing baseline levels for the fatigue strength characterization[11]; in addition, this mode of plotting foreshadows the normalization scheme to be adopted in a later section of the paper. For arbitrary values of applied stress the condition $dK/dc=0$ defines the minimum in Eq. (1), which we designate by asterisk notation:

$$K_* = (r+1)\chi_r P_r / c_*^{r/2} = [(r+1)/r]\psi_r \sigma_a c_*^{1/2} \tag{2a}$$

$$c_* = (r\chi_r P_r / \psi_r \sigma_a)^{2/(r+1)} \tag{2b}$$

The curves with their minimum at M correspond to the special case $K_*=K_c$; at this point we may appropriately identify the critical variables $\sigma_a=\sigma_m$, $c_*=c_m$, i.e.

$$\sigma_m = [r/(r+1)^{(r+1)/r}] K_c^{(r+1)/r} / \psi_r (\chi_r P_r)^{1/r} \tag{3a}$$

$$c_m = [(r+1)\chi_r P_r / K_c]^{2/r} \tag{3b}$$

It may be shown from Eqs. (2) and (3) that

$$K_*/K_c = (\sigma_a/\sigma_m)^{r/(r+1)} \tag{4a}$$

$$c_*/c_m = (\sigma_m/\sigma_a)^{2/(r+1)} \tag{4b}$$

so that as σ_a drops below σ_m the position of the minimum in Fig. 2 displaces downward and to the right relative to M.

The points at which the curves in Fig. 2 intersect the horizontal line $K=K_c$ correspond to equilibrium crack configurations, stable or unstable according to whether the branches have negative or positive slope. The stable equilibria define appropriate initial conditions for ensuing fatigue fracture; c_0 for loading at constant stress rate, c_1 at constant stress. In practice, fatigue effects will be manifest in the postindentation crack configuration before application of tensile loading, causing subcritical extension from c_0 to some nonequilibrium size c_0' (which may or may not exceed c_1). The unstable equilibria at c_f define the final configuration immediately prior to the onset of catastrophic failure. It is useful at this stage to point out that an instability configuration can be achieved without ever departing from an equilibrium state, by steadily increasing the

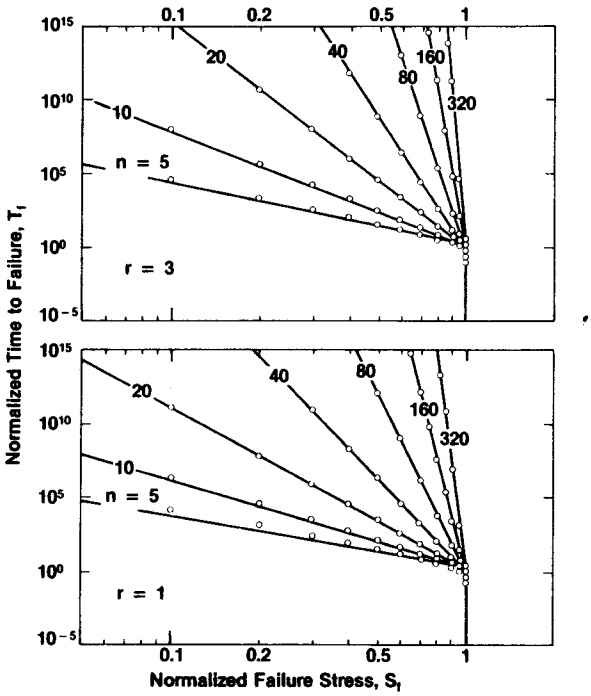

Fig. 3. Normalized plots of lifetime vs failure stress for point and line flaws; static fatigue results. Data points and solid lines represent numerical and analytical solutions of master fatigue differential equation, respectively. Note inert strength cutoff at $S_f=1=S_i$.

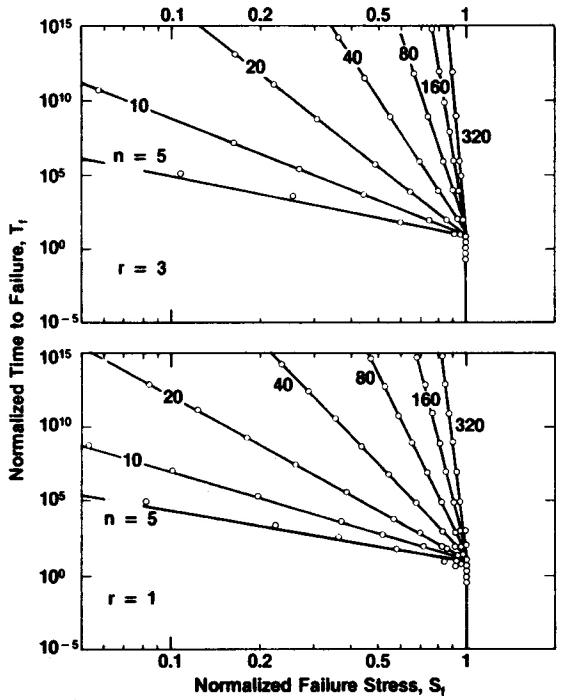

Fig. 4. Normalized plots of lifetime vs failure stress for point and line flaws; dynamic fatigue results. Data points and solid lines represent numerical and analytical solutions, respectively.

applied stress σ_a from zero to σ_m, thereby causing the crack to grow stably from c_0 to c_m; this takes us along $K=K_c$ to point M in Fig. 2, where c_1 merges with c_f to produce spontaneous failure. Since such conditions are most closely met in nonreactive test environments we may define an "inert" strength $\sigma_i=\sigma_m$, which from Eq. (3) can be written in the form

$$\sigma_i=[r/(r+1)]K_c/\psi_r c_m^{1/2} \tag{5}$$

independent of initial crack size.

For comparison, the corresponding inert strength σ_i^0 for Griffith flaws follows from Eq. (1) in the limit of $\chi_r=0$, with spontaneous failure occurring, without any precursor crack growth, at c_i, say:

$$\sigma_i^0=K_c/\psi_r c_i^{1/2} \tag{6}$$

In this case the strength is, of course, sensitive to the initial flaw size; the appropriate value of c_i, i.e. c_0, c_0', or c_1 (or indeed any other such crack dimension), will depend on the nature of the mechanical, thermal, and/or chemical (or other) processes responsible for removing the residual contact field between crack formation and strength testing.

(2) *Formulation and Solution of the Fatigue Equation*

The fracture mechanics approach to the fatigue problem begins with the assumption that a crack velocity function may be written, for a given material/environment system, in the form $v=v(K)$. In combination with the stress intensity factor, $K=K(r, P_r, \sigma_a, c)$, in Eq. (1) and the specified time variation of the applied tensile field, $\sigma_a=\sigma_a(t)$, the velocity function assumes the form of a differential equation, $dc/dt=v[r, P_r, \sigma_a(t), c]$. This equation must be solved for the time-to-failure, t_f, needed to take the crack from c_i to c_f, at which point the stress level defines the fatigue strength, $\sigma_a=\sigma_f$. The primary objective of any such analysis is to determine the relation between σ_f and t_f (or some equivalent parameter, such as stress rate $\dot{\sigma}_a$ in dynamic fatigue).

To proceed with the solution of the differential equation it is necessary, of course, to know the form of the crack velocity function. In this paper we adopt the simple power-law relation

$$v=v_0(K/K_c)^n \tag{7}$$

where v_0 and n are empirical quantities. At the moment, this is the only one of the commonly used crack velocity functions for which we have been able to obtain analytical solutions for flaws with residual stress. Thus we obtain

$$dc/dt=(v_0/K_c^n)\{K[r, P_r, \sigma_a(t), c]\}^n \tag{8}$$

as our master starting equation.

(A) Griffith Flaws; Static and Dynamic Fatigue Solutions: The standard solutions of Eq. (8) for Griffith flaws are well known.[1-3] It is nevertheless instructive to include them here as a base for comparing later solutions. Inserting $\chi_r=0$ into Eq. (1) yields

$$\begin{aligned} dc/dt&=(v_0/K_c^n)K_a^n \\ &=(v_0/K_c^n)[\psi_r\sigma_a(t)c^{1/2}]^n \end{aligned} \tag{9}$$

The problem accordingly reduces to one of straightforward integration by separation of variables. For static fatigue, i.e. $\sigma_a=\text{constant}=\sigma_f$, Eq. (9) becomes simply

$$\int_0^{t_f} dt=[K_c^n/v_0(\psi_r\sigma_f)^n]\int_{c_i}^{c_f} dc/c^{n/2} \tag{10}$$

The integrated result may be written in the form

$$t_f\sigma_f^n=\lambda_s \tag{11}$$

where, in the usual approximation $(c_i/c_f)^{(n-2)/2}\ll 1$, and in conjunction with Eq. (6), we obtain

$$\begin{aligned} \lambda_s&=2K_c^n/(n-2)v_0\psi_r^n c_i^{(n-2)/2} \\ &=[2/(n-2)]\sigma_i^{0n}c_i/v_0 \end{aligned} \tag{12}$$

The appearance of c_i as the controlling crack size in Eq. (12) reflects the fact that the crack system spends the greater proportion of its time evolution to failure in the region of minimum driving force.

The corresponding solution for dynamic fatigue,[1-3] i.e. for $\sigma_a=\dot{\sigma}_a t$ with constant $\dot{\sigma}_a$, can be expressed by the same power law as Eq. (11), but with λ_s replaced by λ_d, where

$$\lambda_d=(n+1)\lambda_s \tag{13}$$

(B) Flaws with Residual Stress; Static Fatigue Solution: For the general case where $\chi_r \neq 0$ in Eq. (1), Eq. (8) becomes

$$dc/dt=(v_0/K_c^n)[K_r+K_a]^n$$
$$=(v_0/K_c^n)[\chi_r P_r/c^{r/2}+\psi_r\sigma_a(t)c^{1/2}]^n \quad (14)$$

Integration by separation of variables is no longer straightforward as it was for Griffith flaws. Even in static fatigue, for which the right side of Eq. (14) contains no explicit terms in time, it is not immediately clear how the failure stress might be extracted from the integral and thereby related to lifetime. It was difficulties of this kind which motivated the numerical approach described in Ref. 11.

However, it can now be demonstrated that Eq. (14) does have an analytical solution at σ_a=constant=σ_f. Since the integrated lifetime is controlled at one extreme by K_r for small cracks ($c \ll c_*$) and at the other extreme by K_a for large cracks ($c \gg c_*$), it is appropriate to introduce a variable that defines the relative stress intensity factor at either extreme. We accordingly choose

$$\xi=K_a/(K_r+K_a)$$
$$=1/[1+(\chi_r P_r/\psi_r\sigma_f)/c^{(r+1)/2}] \quad (15)$$

where ξ defines the fraction of the total stress intensity factor which is associated with the applied field, this fraction increasing monotonically with crack size. A second, important motivation for introducing this reduced variable is to convert the lifetime integral to a dimensionless form so as to display the applied stress and indentation load dependence separately. After considerable manipulation, Eq. (14) becomes

$$\int_0^{t_f} dt=\{[2K_c^n/(r+1)v_0]/[(\psi_r\sigma_f)^{(rn+2)/(r+1)}(\chi_r P_r)^{(n-2)/(r+1)}]\}$$
$$\times\int_{\xi_i}^{\xi_f}\xi^{(rn+2)/(r+1)-1}(1-\xi)^{(n-2)/(r+1)-1}d\xi \quad (16)$$

and we note that σ_f does indeed appear outside the integral. At this stage a significant simplification in the expression can be made by introducing the quantity

$$n'=(rn+2)/(r+1) \quad (17)$$

This will be seen later, with the benefit of hindsight, to be a particularly convenient choice of substitution. A further simplification is to assign the following values to the limits of integration in Eq. (16), consistent with our identification of the initial and final conditions in Fig. 2 and Eq. (15),

$$\xi_i=\psi_r\sigma_f c_i^{1/2}/K_c \to 0 \quad (18a)$$

$$\xi_f=\psi_r\sigma_f c_f^{1/2}/K_c \to 1 \quad (18b)$$

in which case the integral in Eq. (16) reduces to the beta function.* These value assignments are tantamount to saying that the initial conditions are governed by the residual component of the stress intensity factor, the final conditions likewise by the applied component. In any case, the final result is not expected to be sensitive to the limits of integration, bearing in mind that the region of minimum driving force in Fig. 2, which must control the fracture kinetics, lies intermediate to the initial and final configurations. This assumption is verified in the Appendix. With these simplifications Eq. (16) reduces to

$$t_f=[2K_c^n/(r+1)v_0(\psi_r\sigma_f)^{n'}(\chi_r P_r)^{n-n'}]B(n', n-n') \quad (19)$$

with the beta function

$$B(n', n-n')=\int_0^1 \xi^{n'-1}(1-\xi)^{(n-n')-1}d\xi \quad (20)$$

Thus the requisite relation between lifetime and failure stress has the familiar form

$$t_f\sigma_f^{n'}=\lambda_s' \quad (21)$$

*See any standard text on advanced mathematical methods.

where we obtain, in conjunction with Eqs. (3) and (5),

$$\lambda_s'=[2K_c^n/(r+1)v_0\psi_r^{n'}(\chi_r P_r)^{n-n'}]B(n', n-n')$$
$$=\{[2(r+1)^{n-1}/r^{n'}]B(n', n-n')\}\sigma_i^{n'}c_m/v_0$$
$$\cong[8\pi/(r+1)n']^{1/2}\sigma_i^{n'}c_m/v_0 \quad (22)$$

the last expression arising from an asymptotic expansion of the beta function for large n' (Appendix).

While the form of Eq. (21) is indistinguishable from that of Eq. (11) for Griffith flaws, the exponent and coefficient are significantly modified. The implications of these modifications are discussed in Section IV.

III. Comparison of Analytical and Numerical Solutions: Extension to Constant Stress-Rate Loading

It is instructive to examine the mutual consistency of the results obtained analytically in Section II and numerically in Ref. 11. To do this, and to broaden the scope of the treatment to date, numerical solutions, previously confined to the special case $\dot{\sigma}_a$=constant and r=3,[11] are here generated for each combination of fatigue (static or dynamic) and flaw (point or line) types.

Following Ref. 11, reduced variables are introduced as follows:

$$S_a=\sigma_a/\sigma_m \quad (23a)$$

$$C=c/c_m \quad (23b)$$

$$T=tv_0/c_m \quad (23c)$$

Reference to Eq. (5) then allows the differential equation for flaws with residual stress, Eq. (14), to be expressed in a more universal form,

$$dC/dT=\{1/(r+1)C^{r/2}+[r/(r+1)]S_a(T)C^{1/2}\}^n \quad (24)$$

which is especially amenable to numerical analysis. This equation is solved by a stepwise integration procedure for the (reduced) time-to-failure T_f to take the crack from C_i (approximated by the value $C_0=1/(r+1)^{2/r}$ at $S_a=0$) to C_f.[11] The corresponding failure stress S_f at the critical end point of the integration is seen to be uniquely determined by the values of r and n and the form of the stressing function $S_a(T)$. It is noted that the normalization scheme conveniently relates all variables to the inert strength state, i.e. $S_i=S_m=1$ and $C_m=1$, as represented by the reference point M in Fig. 2.

To facilitate the required comparisons, let us translate the essential results of the analytical treatment in Section II into reduced variable notation. Taking static fatigue first, i.e. S_a=constant=S_f, Eq. (21) retains its basic form,

$$T_f S_f^{n'}=\Lambda_s' \quad (25)$$

with the coefficient relating to its counterpart in Eq. (22) as

$$\Lambda_s'=\lambda_s' v_0/\sigma_i^{n'}c_m$$
$$=[2(r+1)^{n-1}/r^{n'}]B(n, n-n')$$
$$\cong[8\pi/(r+1)]^{1/2}/n'^{1/2} \quad (26)$$

where the last line in this equation is an asymptotic approximation in n' (Appendix).

At this point, it is pertinent to recall the essential equivalence of the static fatigue solutions for flaws with and without residual stress, Eqs. (21) and (11). It would appear reasonable to expect this equivalence to extend to dynamic fatigue, $S_a=\dot{S}_a T$ ($\dot{S}_a$ constant). Accordingly, since in the case of Griffith flaws the static and dynamic solutions can be shown analytically to have exponents which are identical and coefficients which relate linearly via Eq. (13), we may proceed by analogy and modify Eq. (25), thus

$$T_f S_f^{n'}=\Lambda_d' \quad (27)$$

where we have from Eq. (26)

$$\Lambda_d'=\lambda_d' v_0/\sigma_i^{n'}c_m=(n'+1)\Lambda_s'\cong[8\pi/(r+1)]^{1/2}n'^{1/2} \quad (28)$$

with the same asymptotic approximation as made in Eq. (26).

Figures 3 and 4 show the results of both analytical and numerical

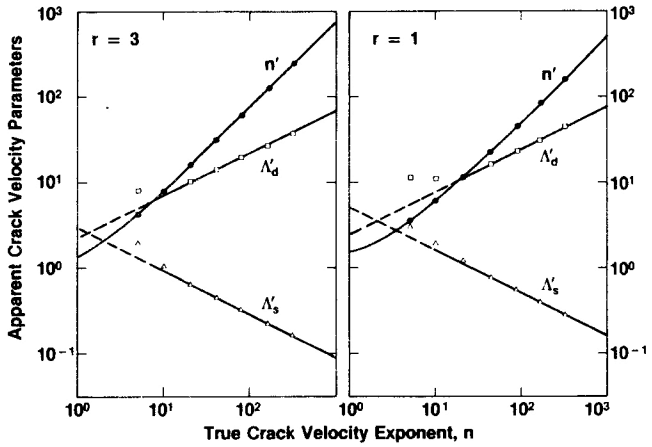

Fig. 5. Plots showing variation of exponent n' (n'_s and n'_d cannot be distinguished in these plots) and coefficients Λ'_s and Λ'_d with n, for point and line flaws. Data points and solid lines represent numerical and analytical evaluations, respectively.

calculations on logarithmic plots of lifetime vs failure stress for static and dynamic fatigue, respectively, and for point and line flaws. The data points in these plots are numerical evaluations of Eq. (24) at either fixed S_a (Fig. 3) or $\dot{S}_a$ (Fig. 4) for selected values of n. The corresponding solid lines are analytical representations of Eqs. (25) and (27), in conjunction with Eq. (17). The degree of correlation between data points and solid curves reflects the accuracy of the theory developed in Section II. In this context the tendency for systematic departures to increase at low n (or n') values may be taken as a measure of the range of validity of the asymptotic beta function expansion used in the evaluation of the integral in Eq. (16). Special note may be made of the fact that the correlations appear to be as strong for the dynamic fatigue results in Fig. 4 as for the static fatigue in Fig. 3, thereby providing some justification for the equivalence argument adopted to extend the theoretical analysis earlier in this section.

A more detailed comparison of results is obtained by considering the specific variations of the exponent n' and coefficients Λ' in Eqs. (25) and (27) with n. This is done in Fig. 5 for point and line flaws. The data points again represent numerical evaluations of Eq. (24), obtained from slope and intercept evaluations in the "linear" region of the lifetime vs failure stress plots; the solid curves likewise represent analytical evaluations from Eqs. (17), (26), and (28). The disagreement between the two approaches is $<1\%$ for the exponent and $<10\%$ for the coefficients in the domain $n>10$.

IV. Discussion

The formulation presented in this paper demonstrates that analytical solutions can be obtained to the fracture mechanics fatigue equations for flaws which are subject to residual-contact driving forces and which extend according to a power-law crack velocity function. A major feature of these solutions is the fact that they are identical in basic form to those obtained for Griffith flaws in conventional fatigue analysis. Thus, from a standard linear plot of lifetime vs failure stress in logarithmic coordinates it would not be possible to determine, without independent information on the crack velocity parameters, whether the flaws in a given material/environment system are or are not influenced by residual stresses. This conclusion should provide some comfort to those who have advocated the exclusive use of strength data for predicting component lifetimes, since the nature of the flaw now does not enter into consideration (unless perhaps the predictions require extrapolation beyond the data range[10]). Of particular importance in this context is the widely proposed use of dynamic fatigue testing as the source of base data for design requirements; in terms of a lifetime vs failure stress diagram the curve for static loading generates from that for dynamic loading via a simple connecting relation for the intercepts. To illustrate, Fig. 6 shows data from both dynamic[9] and static[10] fatigue test runs on indented soda-lime glass in water. A least-squares fit through the dynamic fatigue data gives n', Eq. (27); subsequent translation downward through $\log(n'+1)$, Eq. (28), generates the static fatigue curve. The agreement between prediction and observation in the latter case, notwithstanding the experimental scatter, may be taken as a justification for the "equivalence" argument used to infer the existence of Eqs. (27) and (28) from their Griffith counterparts, Eqs. (11) and (13).

There is, however, considerable danger in analyzing fatigue results from materials whose flaw characteristics are not known. This is particularly so if one attempts to relate the strength data to the parameters in the crack velocity function. The point is most readily demonstrated by considering the exponent in this function in terms of the slope of lifetime vs failure stress plot. From Eq. (11) for Griffith flaws the slope gives n (more strictly, its negative) directly, whereas from Eq. (21) for flaws with residual stress the corresponding slope is n'; in the latter case evaluation of the true exponent requires inversion of Eq. (17);

$$n=4n'/3-2/3 \qquad (r=3) \tag{29a}$$

$$n=2n'-2 \qquad (r=1) \tag{29b}$$

Thus substantial errors may be incurred if the conventional theory of fatigue is used to analyze data for contact-induced flaws which have undergone no subsequent stress relaxation. For example, in Fig. 6 the apparent exponent is determined at $n'=13.7\pm0.2$, whence Eq. (29*a*) appropriate to point (Vickers-induced) flaws predicts $n=17.6\pm0.3$; this latter value is close to the true exponent $n=17.9\pm0.5$ obtained from comparative tests on indented specimens subjected to an anneal treatment prior to strength testing,[9] and lies in the range of $16<n<19$ generally found for large-scale cracks in the system soda-lime-glass/water.[16] The discrepancy between apparent and true exponents is predicted to be even greater for linear flaws, almost a factor of 2, Eq. (29*b*). It is interesting to note that discrepancies of this order were found by Pletka and Wiederhorn[17] in certain ceramics where machining damage provided the strength-controlling flaws.

Similar care must be exercised in evaluating the coefficient of the crack velocity function from the intercept on a fatigue plot. For flaws with residual stress, inversion of Eqs. (26) and (28) gives

$$v_0=\Lambda'\sigma_i^{n'}c_m/\lambda' \tag{30}$$

where

$$\Lambda'=(2\pi/n')^{1/2} \qquad (\sigma_a=\text{constant}, r=3) \tag{31a}$$

$$\Lambda'=(4\pi/n')^{1/2} \qquad (\sigma_a=\text{constant}, r=1) \tag{31b}$$

$$\Lambda'=(2\pi n')^{1/2} \qquad (\dot{\sigma}_a=\text{constant}, r=3) \tag{31c}$$

$$\Lambda'=(4\pi n')^{1/2} \qquad (\dot{\sigma}_a=\text{constant}, r=1) \tag{31d}$$

Inversion of the corresponding intercept relations for Griffith flaws, Eqs. (12) and (13), leads to an analogous result, but with a different Λ' term and with c_i replacing c_m as the controlling crack parameter.

We should emphasize here that Eq. (31) represents only a first-order approximation; additional terms in a series expansion may be required where accuracy requirements are stringent (Appendix). However, since lifetimes are generally plotted in logarithmic coordinates the present approximation will usually suffice, except perhaps at $n\lesssim10$.

This sensitivity of the slope and intercept terms in the fatigue relations to the nature of the strength-controlling flaw provides a strong case for the use of indentation testing in the evaluation of crack velocity parameters. Any uncertainty as to whether the cracks are subject to residual stress effects and whether the cracks have essential point or line (or intermediate) geometry is then eliminated. Of course, such elements of uncertainty can hardly be avoided in ceramic components which are to be placed in service, so any attempt to apply the above procedure in reverse, i.e. to use macroscopically determined crack velocity parameters to predict lifetime characteristics, needs to be treated with extreme caution.

Indeed, the present results would appear to strengthen the case for fatigue testing on the actual surface finish to be used in service.

Thus far in the discussion we have effectively been considering the fatigue response of a given material/environment system at fixed indentation loading conditions. How might the formalism developed here be rearranged to accommodate a test program which calls for the removal of these restrictions? Ideally, it would be convenient to be able to devise a scheme whereby all data for a given system could be plotted onto a universal curve, regardless of load, such that comparative evaluations could be readily made for different materials. Alternatively, one could use load as a control variable for investigating the effect of flaw size on the validity of crack growth laws.[18] Accordingly, inserting Eq. (30) into the general fatigue relation $t_f\sigma_f^{n'}=\lambda'$ gives[†]

$$t_f''/\Lambda' c_m=(1/v_0)(\sigma_i/\sigma_f)^{n'} \tag{32}$$

The load P_r may now be introduced explicitly into the analysis via Eq. (3) by writing

$$\sigma_i=\sigma_m=\zeta/P_r^{1/r} \tag{33a}$$

$$c_m=\eta P_r^{2/r} \tag{33b}$$

where $\zeta=\zeta(r, \chi_r, \psi_r, K_c)$ and $\eta=\eta(r, \chi_r, K_c)$ are experimentally measurable inert-strength constants.[12] Then Eq. (32) becomes

$$t_f/P_r^{2/r}=(\Lambda'\zeta^{n'}\eta/v_0)/(\sigma_f P_r^{1/r})^{n'} \tag{34}$$

so plots of $t_f/P_r^{2/r}$ vs $\sigma_f P_r^{1/r}$ in logarithmic coordinates should produce universal straight lines for individual material/indenter systems. These plots are, of course, nothing more than generalized versions of those illustrated in Fig. 6. The advantage of this scheme is that it provides the basis for constructing "master diagrams" in which the relative fracture properties of different materials are immediately apparent. Thus the slope of any such plot in the fatigue region gives a direct measure of the "susceptibility" to delayed failure, in the manner already discussed in relation to Fig. 6; the inert-strength cutoff likewise gives a measure of the intrinsic "toughness," as reflected by the parameter ζ in Eq. (33*a*). Clearly, the materials with superior strength characteristics will be those which, for a specified lifetime domain, lie to the right of the diagram. Further details of this proposed scheme will be explored elsewhere.[19]

There are in the analysis several implicit assumptions which have not been given close attention in the body of the text. These include: (*a*) that the solutions of the fatigue differential equations are insensitive to initial conditions, (*b*) that the multiple-region effects in the crack velocity function are negligible, (*c*) that the test material is free of preexisting surface stresses. Reference 11 contains a detailed discussion of these points.

Finally, although our attention has focused on indentation cracks, the basic stress intensity formulation of Eq. (1) might be expected to cover a far broader range of flaw types. Similarities in the local residual stress fields about microstructural defects in ceramics (due to strain incompatibilities at grain or inclusion boundaries) and indentations have already been noted by Green.[15] Extension to these other cases is accordingly a simple matter of reinterpreting the physical meaning of the quantity $\chi_r P_r$ in Eq. (15) in terms of characteristic pressure and radius parameters which define the intensity and extent of the field.[8] Then, provided of course that the reactive chemical species has access to the defect centers to cause fatigue in the first place, the conventional analysis of lifetime properties is subject to precisely the same modifications as described for contact flaws in Sections II and III.

[†]It may be noted in passing that if we were to define a dimensionless velocity $v=\Lambda' c_m/t_f$ and stress intensity factor $K=\sigma_f/\sigma_i$, Eq. (32) could be inverted to give $v=v_0K^{n'}$. In this interpretation the plotting scheme to be proposed may be regarded as representative of an inverse crack velocity function.

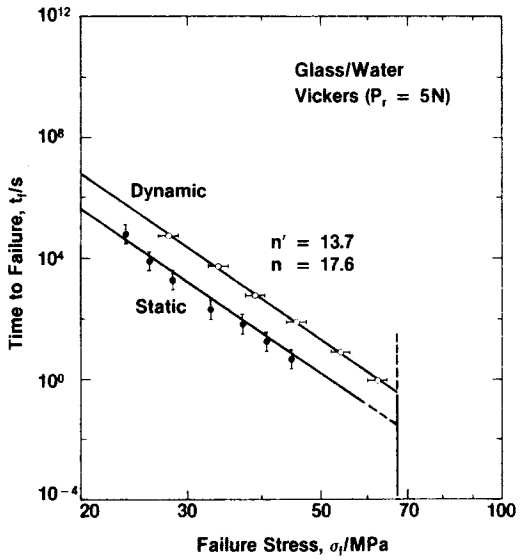

Fig. 6. Plot comparing static and dynamic fatigue response for soda-lime glass in water using indentation flaws. Data from Refs. 9 and 10, standard deviation error bars.

APPENDIX

Lifetime Integral and its Approximations

In this appendix the assumptions made in the derivation of the lifetime formulation for cracks in combined residual and applied stress fields are examined. Specific attention is directed to the dimensionless quantity in Eq. (26),

$$\Lambda_s'=[2(r+1)^{n-1}/r^{n'}]\int_{\xi_i}^{\xi_f}\xi^{n'-1}(1-\xi)^{n-n'-1}d\xi \tag{A-1}$$

where the integral is the generalized version of Eq. (20) (i.e. with variable limits of integration). Consideration of this one expression is sufficient to cover all the approximations referred to in Sections II(2*B*) and III. The treatment here is taken in two parts: in the first, Λ_s' is expressed in terms of the beta function and two incomplete beta functions, and these functions are evaluated to determine their relative importance; in the second part, the beta function, which is confirmed to be the dominant term in Λ_s', is expanded in an asymptotic series for large values of n.

An important point to keep in mind here is that accuracy in Λ_s', although clearly desirable, is not nearly as critical as it is in the exponent n' in Eq. (25), for which we have an exact expression (Eq. (17)). Generally, accuracy to within a factor of two in Λ_s' is adequate for most lifetime and crack velocity evaluations.

(1) Beta Function Expression

The integral in Eq. (A–1) may be rewritten as follows:

$$\int_{\xi_i}^{\xi_f}\xi^{n'-1}(1-\xi)^{n-n'-1}d\xi=\int_0^1\xi^{n'-1}(1-\xi)^{n-n'-1}d\xi - \int_0^{\xi_i}\xi^{n'-1}(1-\xi)^{n-n'-1}d\xi - \int_{\xi_f}^1\xi^{n'-1}(1-\xi)^{n-n'-1}d\xi \tag{A-2}$$

The first integral is the beta function $B(n', n-n')$ as previously defined in Eq. (20). The second and third integrals are the incomplete beta functions[20] $B_{\xi_i}(n', n-n')$ and $B_{(1-\xi_f)}(n-n', n')$ (using a transformation of variables $\xi\rightarrow 1-\xi'$ in the latter case). Equation (A–1) then becomes

$$\Lambda_s'=[2(r+1)^{n-1}/r^{n'}]\,[B(n', n-n') - B_{\xi_i}(n', n-n') - B_{(1-\xi_f)}(n-n', n')] \tag{A-3}$$

Table IA. Initial and Final Values of Reduced Stress Intensity Factor, $\xi=K_a/K$, for Selected Values of Reduced Applied Stress, $S_a=\sigma_a/\sigma_m$

Flaw type	S_a	ξ_i	ξ_f
Point ($r=3$)	0.9	0.559	0.891
	0.7	0.390	0.959
	0.5	0.261	0.986
	0.3	0.150	0.997
	0.1	0.048	1.000
Line ($r=1$)	0.9	0.342	0.658
	0.7	0.226	0.774
	0.5	0.146	0.854
	0.3	0.082	0.918
	0.1	0.026	0.974

Table IIA. Comparison of Λ_s' Evaluations from Equation (A–3) Using Beta Function Contribution Only and Full Expression

Flaw type	n	n'	Λ_s' (beta)	S_a	Λ_s'
Point ($r=3$)	10	8	1.110	0.9	0.780
				0.7	1.051
				0.3	1.110
	18	14	0.755	0.9	0.659
				0.7	0.751
				0.5	0.755
	38	29	0.492	0.9	0.482
				0.7	0.492
Line ($r=1$)	10	6	2.032	0.9	1.181
				0.7	1.768
				0.1	2.032
	18	10	1.348	0.9	1.045
				0.7	1.315
				0.3	1.348
	38	20	0.864	0.9	0.813
				0.7	0.864

The beta function in Eq. (A–3) is readily computed from the more familiar gamma function to which it is related[20]; generally,

$$B(n', n-n')=\Gamma(n')\Gamma(n-n')/\Gamma(n) \qquad (A\text{–}4a)$$

or, more simply, when both n and n' are integers,

$$B(n', n-n')=(n'-1)!(n-n'-1)!/(n-1)! \qquad (A\text{–}4b)$$

Computation of the *incomplete* beta functions, however, requires prior specification of the reduced quantities ξ_i and ξ_f. In the same way as the limiting values of these two quantities in Eq. (18) are derived from the defining relation Eq. (15), we may write,

$$\xi=[r/(r+1)]S_aC^{1/2} \qquad (A\text{–}5)$$

where we have invoked the normalizing scheme of Eq. (23). For present purposes we can adequately illustrate the approximations involved by considering the relatively simple case of static fatigue, i.e. S_a=constant; values of ξ_i and ξ_f appropriate to initial and final crack sizes are then obtained from the roots of Eq.(1) at $K=K_c$ (again expressed in normalized form). Table IA shows values for several reduced applied stresses for both point and line flaws. These values can clearly differ substantially from the limits of $\xi_i=0$ and $\xi_f=1$ of Eq. (18), particularly at stress levels approaching the inert strength $S_a=1$.

In our study the incomplete beta functions have been evaluated using an adaptive Simpson's rule computer code for the integration limits of Table IA, although algorithms are available for analytical (but tedious) computation.

Table IIA summarizes the results of the calculations, for selected values of n and for point and line flaws. The tabulation compares evaluations of Λ_s' made with the incomplete beta functions omitted and included. It is clear that the terms containing these incomplete beta functions make a significant contribution only at low n and high S_a. Even in these worst cases the discrepancy is generally likely to be less than the factor of two tolerance level quoted earlier. Thus in the region of larger n (which appears to pertain to most practical ceramics) and long lifetimes, Λ_s' effectively becomes an invariant quantity, independent of applied stress.

Table IIIA. Comparison of Λ_s' Evaluations from Equation (A–9) Using Lead Term and Full Beta Function Expression

Flaw type	n	n'	$[8\pi/(r+1)n']^{1/2}$	Λ_s' (beta)
Point ($r=3$)	10	8	0.886	1.110
	18	14	0.670	0.755
	38	29	0.465	0.492
	78	59	0.326	0.335
	158	119	0.230	0.233
Line ($r=1$)	10	6	1.447	2.032
	18	10	1.121	1.348
	38	20	0.793	0.864
	78	40	0.560	0.584
	158	80	0.396	0.405

(2) Asymptotic Expansion of Beta (Gamma) Function

In the spirit of the approximations above in which only the beta function is retained in Eq. (A–3) we have

$$\Lambda_s'=[2(r+1)^{n-1}/r^{n'}]\Gamma(n')\Gamma(n-n')/\Gamma(n) \qquad (A\text{–}6)$$

The gamma functions in this expression may now be expanded using Stirling's formula[20]; e.g. for the first gamma function

$$\ln \Gamma(n')\sim \ln (2\pi/n')^{1/2}+n' \ln n'-n'+S(n') \qquad (A\text{–}7)$$

where $S(n')$ is the series

$$S(n')=\sum_{k=1}^{\infty}[B_{2k}/2k(2k-1)]/n'^{2k-1} \qquad (A\text{–}8)$$

with B_{2k} the Bernoulli numbers ($B_2=1/6$, $B_4=-1/30$, etc.).[20] After some manipulation, Eq. (A–6) reduces to

$$\ln \Lambda_s'\sim \ln [8\pi/(r+1)n']^{1/2} + n' \ln [n'/(n'-2)]-(n-1/2) \ln [n/(n-2)] + S(n')-S(n)+S(n-n') \qquad (A\text{–}9)$$

In this expression the second and third terms tend to cancel and the series S terms become small as n increases, leaving the lead term as the dominant quantity. The accuracy with which this lead term can be used to represent Λ_s' may be gauged from Table IIIA.

Acknowledgments: The authors thank T. J. Chuang and E. D. Case for assistance with the calculations in the Appendix.

References

[1] S. M. Wiederhorn; pp. 613–46 in Fracture Mechanics of Ceramics, Vol. 2. Edited by R. C. Bradt, D. P. H. Hasselman, and F. F. Lange. Plenum, New York, 1974.
[2] A. G. Evans and S. M. Wiederhorn, "Proof Testing of Ceramic Materials: An Analytical Basis for Failure Prediction," *Int. J. Fract.*, **10** [3] 379–92 (1974).
[3] S. M. Wiederhorn and J. E. Ritter; pp. 202–14 in Fracture Mechanics Applied to Brittle Materials. Edited by S. W. Frieman. *ASTM Spec. Tech. Publ.*, No. **678**, 1979.
[4] A. A. Griffith, "Phenomena of Rupture and Flow in Solids," *Philos. Trans. R. Soc. (London) Ser. A.*, **221** [4] 163–98 (1920).
[5] B. R. Lawn and T. R. Wilshaw, Fracture of Brittle Solids; Chs. 2 and 3. Cambridge University Press, London, 1975.
[6] A. H. Cottrell, "Theory of Brittle Fracture in Steel and Similar Metals," *Trans. Met. Soc.*, **212** [3] 192–203 (1958).
[7] (*a*) D. B. Marshall and B. R. Lawn, "Residual Stress Effects in Sharp-Contact Cracking: I," *J. Mater. Sci.*, **14** [8] 2001–12 (1979).
(*b*) D. B. Marshall, B. R. Lawn, and P. Chantikul, "Residual Stress Effects in Sharp-Contact Cracking: II," *J. Mater. Sci.*, **14** [9] 2225–35 (1979).
[8] B. R. Lawn, A. G. Evans, and D. B. Marshall, "Elastic/Plastic Indentation Damage in Ceramics: The Median/Radial Crack System," *J. Am. Ceram. Soc.*, **63** [9–10] 574–81 (1980).
[9] D. B. Marshall and B. R. Lawn, "Flaw Characteristics in Dynamic Fatigue: The Influence of Residual Contact Stresses," *J. Am. Ceram. Soc.*, **63** [9–10] 532–36 (1980).

[10]P. Chantikul, B. R. Lawn, and D. B. Marshall, "Micromechanics of Flaw Growth in Static Fatigue: Influence of Residual Contact Stresses," *J. Am. Ceram. Soc.*, **64** [6] 322–25 (1981).
[11]B. R. Lawn, D. B. Marshall, G. R. Anstis, and T. P. Dabbs, "Fatigue Analysis of Brittle Materials Using Indentation Flaws: I," *J. Mater. Sci.*, **16** [10] 2846–54 (1981).
[12]R. F. Cook, B. R. Lawn, and G. R. Anstis, "Fatigue Analysis of Brittle Materials Using Indentation Flaws: II," *J. Mater. Sci.*, **17** [4] 1108–16 (1982).
[13]D. B. Marshall; unpublished work.
[14]D. B. Marshall and B. R. Lawn, "Residual Stresses in Dynamic Fatigue of Abraded Glass," *J. Am. Ceram. Soc.*, **64** [1] C-6–C-7 (1981).
[15]D. J. Green, in Fracture Mechanics of Ceramics. Edited by R. C. Bradt, D. P. H. Hasselman, F. F. Lange, and A. G. Evans. Plenum, New York, 1982.
[16]S. M. Wiederhorn; unpublished work.
[17]B. J. Pletka and S. M. Wiederhorn, "A Comparison of Failure Predictions by Strength and Fracture Mechanics Techniques," *J. Mater. Sci.*, **17** [5] 1247–68 (1982).
[18]T. D. Dabbs, B. R. Lawn, and P. L. Kelly, "A Dynamic Fatigue Study of Soda-Lime and Borosilicate Glasses Using Small-Scale Indentation Flaws," *Phys. Chem. Glasses*, **23** [2] 58–66 (1982).
[19]R. F. Cook and B. R. Lawn; unpublished work.
[20]I. S. Gradshteyn and I. M. Ryzhik, Table of Integrals, Series and Products; Chs. 8, 9. Academic Press, New York, 1980.